Published in final edited form as:
J Biol Inorg Chem. 2011 March ; 16(3): 373–380. doi:10.1007/s00775-010-0733-z.

Rates of intercalator-driven platination of DNA determined by a restriction enzyme cleavage inhibition assay

Jayati Roy Choudhury, **Lu Rao**, and **Ulrich Bierbach**
Department of Chemistry, Wake Forest University, Winston-Salem, NC 27109, USA

Abstract

A restriction enzyme cleavage inhibition assay was designed to determine the rates of DNA platination by four non-cross-linking platinum–acridine agents represented by the formula $[Pt(am_2)LCl](NO_3)_2$, where am is a diamine nonleaving group and L is an acridine derived from the intercalator 1-[2-(acridin-9-ylamino)ethyl]-1,3-dimethylthiourea (ACRAMTU). The formation of monofunctional adducts in the target sequence 5′-CGA was studied in a 40-base-pair probe containing the **Eco**RI restriction site GAATTC. The time dependence of endonuclease inhibition was quantitatively analyzed by polyacrylamide gel electrophoresis. The formation of monoadducts is approximately 3 times faster with double-stranded DNA than with simple nucleic acid fragments. Compound **1** (am_2 is ethane-1,2-diamine, L is ACRAMTU) reacts with a first-order rate constant of $k_{obs} = 1.4 \pm 0.37 \times 10^{-4}$ s^{-1} ($t_{1/2} = 83 \pm 22$ min). Replacement of the thiourea group in ACRAMTU with an amidine group (compound 2) accelerates the rate by fourfold ($k_{obs} = 5.7 \pm 0.58 \times 10^{-4}$ s^{-1}, $t_{1/2} = 21 \pm 2$ min), and introduction of a propane-1,3-diamine nonleaving group results in a 1.5-fold enhancement in reactivity (compound **3**, $k_{obs} = 2.1 \pm 0.40 \times 10^{-4}$ s^{-1}, $t_{1/2} = 55 \pm 10$ min) compared with the prototype. Derivative **4**, containing a 4,9-disubstituted acridine threading intercalator, was the least reactive compound in the series ($k_{obs} = 1.1 \pm 0.40 \times 10^{-4}$ s^{-1}, $t_{1/2} = 104 \pm 38$ min). The data suggest a correlation may exist between the binding rates and the biological activity of the compounds. Potential pharmacological advantages of rapid formation of cytotoxic monofunctional adducts over the common purine–purine cross-links are discussed.

Keywords

Platinum–acridine agents; Monofunctional adducts; DNA binding; Kinetics; Gel electrophoresis

Introduction

Nuclear DNA is the primary pharmacological target of platinum-based anticancer drugs. The antitumor effect of these agents is caused by irreversible adducts formed with DNA bases [1,2]. Cisplatin (*cis*-diamminedichloridoplatinum(II), *cis*-$[PtCl_2(NH_3)_2]$) and its second-generation derivatives induce cross-links (mainly intrastrand) in DNA, which, if not repaired, trigger apoptotic cell death [2]. Thus, the ability of these drugs to reach the nucleus and irreversibly cross-link DNA bases is crucial for their antitumor activity. DNA adduct levels and adduct repair have been demonstrated to correlate with the cytotoxic potential of

bierbau@wfu.edu .

Electronic supplementary material The online version of this article (doi:10.1007/s00775-010-0733-z) contains supplementary material, which is available to authorized users.

cisplatin and are being used as prognostic markers of clinical outcome in patients receiving platinum drugs [3–6]. One goal in platinum-based chemotherapy, therefore, is to design novel agents with improved target affinity and selectivity. This can be achieved, for instance, by varying the ligand set on platinum to tune the reactivity of the metal or by incorporating DNA-affinic carrier groups into the complex [7,8].

Platinum-acridine conjugates are a novel class of DNA-targeted agents with potent activity in chemoresistant cancers in vitro and in vivo. The class is represented by the parent compound [PtCl(en)(ACRAMTU)]$(NO_3)_2$ (en is ethane-1,2-diamine, ACRAMTU is 1-[2-(acridin-9-ylamino)ethyl]-1, 3-dimethylthiourea; compound **1**, Fig. 1) [9,10]. The DNA-binding mechanisms of **1** and cisplatin differ in many important ways. The design of **1** aimed to generate a non-cross-linking platinating agent whose “covalent” DNA interactions would be dominated by a sequence- and groove-specific intercalator-based carrier [9,10]. The rationale behind this approach was that the unique binding mechanism would lead to adducts that are recognized and processed by the cell differently from those formed by cisplatin. Using a combination of spectroscopic, analytical, and biochemical techniques, as well as high-resolution methods, we demonstrated that **1** forms monofunctional adducts with guanine and adenine at the preferred intercalation sites of the acridine carrier, most prominently in the sequences 5′-CG, 5′-GA, and 5′-TA [11–13]. This contrasts with the damage profile of cisplatin, which has a high affinity for runs of contiguous guanines [14].

Compound **1** binds to native double-stranded DNA (dsDNA) significantly faster than cisplatin, and platination is virtually complete after 6 h [12,15]. By contrast, in mononucleotide model systems, **1** reacts more sluggishly than cisplatin under the same conditions [11,16,17]. These findings suggest that reactions using simple nucleic acid fragments, although useful in determining the relative reactivities of structurally related platinum derivatives with nucleobase nitrogen, have limitations in modeling the interactions of platinum–intercalator compounds with biologically relevant dsDNA. To study the time course of platinum binding to dsDNA, various techniques have been employed. Atomic absorption and emission spectrophotometry, as well as electroanalytical methods, in particular atomic emission and absorption spectrometry, are typically used to monitor the progress of platination, based on global binding levels in random-sequence DNA [18]. Unfortunately, these methods do not provide any insight into the rate of adduct formation at specific target sites. Two-dimensional heteronuclear NMR spectroscopy has been exploited to gain insight into mechanistic details of the formation of site-specific adducts in short model duplexes, such as the nature of reaction intermediates [19–21]. Here, we have used a restriction enzyme cleavage inhibition assay to determine the rates of monofunctional adduct formation of **1** and three of its second-generation derivatives (compounds **2–4**,Fig. 1) at a common high-affinity site targeted by these agents. The gel-based assay, which has previously been used to assess differences in the DNA binding levels of compounds **1** and **2** [22], proves to be a powerful, sensitive technique for probing the effects of subtle structural alterations of the parent complex on the kinetics of DNA platination. The results suggest a relationship may exist between the DNA-binding efficiency and the biological activity of platinum–acridines in rapidly proliferating cancer cells.

Materials and methods

Materials

Complexes **1**–**4** were synthesized as described previously [22–25]. Stock solutions of all compounds were prepared in 10 mM tris(hydroxymethyl)aminomethane (Tris)–HCl buffer (pH 7.5), and concentrations were determined by UV–vis spectrophotometry using published absorptivities [22–25]. (Electrospray mass spectra were recorded in positive-ion mode of the Tris–HCl-buffered solutions to confirm that Tris does not react with platinum

under the incubation conditions of this assay. Likewise, no aquated platinum species were detected, confirming that the monochlorido complexes are relatively inert toward chloride exchange in this medium [17].) Biochemical-grade chemicals were used for the preparations of all buffers and reagents. The single-stranded DNA fragments 5′-GCAGCTGGCAATGGGTCGAATTCGCAGCTGGCAATGGGTC-3′ (top strand) and 5′-GACCCATTGCCAGCTGCGAATTCGACCCATTGCCAGCTGC-3′ (bottom strand) were synthesized and purified by high-performance liquid chromatography (IDT, Coralville, IA, USA).

Incubations and polyacrylamide gel separations

Incubations of complexes **1**–**4** with the probe sequence were performed and reactions quenched using conditions described previously [22]. The top strand was radioactively labeled at the 5′-end using T4 polynucleotide kinase (Epicentre Biotechnologies, Madison, WI, USA) and [γ-^{32}P]ATP (Amersham Biosciences, Piscataway, NJ, USA) and annealed with the complementary strand by incubating both strands at 95 °C for 5 min and subsequently cooling the solutions to room temperature in a dry bath. Reactions were performed in 10 mM Tris–HCl buffer (pH 7.5) in a volume of 225 μL containing 0.55 μM ^{32}P-labeled DNA probe and 4.4 μM platinum complex, from which 25 μL was withdrawn at each time point and incubated with thiourea (fivefold excess relative to platinum complex) at 4 °C for 30 min. Platinum-treated DNA samples were exhaustively dialyzed against Tris–HCl buffer at 4 °C for 12 h using MINI dialysis units (molecular mass cutoff 3,500 Da; Pierce Biotechnology, Rockford, IL, USA) to remove excess thiourea and unbound platinum complex. Reaction products were subsequently digested with 60 units of *Eco*RI (New England Biolabs, Beverly, MA, USA) at 37 °C for 40 min in reaction buffer provided by the vendor and loaded directly onto denaturing (12% acrylamide, 8 M urea) polyacrylamide gels. Electrophoretic separations were carried out for 60 min at 170 V.

Kinetic analysis

Bands on the gels were integrated using Quantity One (version 4.4.1; Bio-Rad, Hercules, CA, USA). The intensities of the bands were normalized relative to the total intensity across each lane. Relative band intensities calculated for the full-length fragments were plotted versus incubation time and fitted to the functional form

$$y = a\left(1 - e^{-bx}\right), \tag{1}$$

where y represents [DNA*f.-l.*]$_t$/[DNA$_{tot}$] (where f.-l. is full length), a represents [DNA$_{f.-l.}$]$_{max}$/[DNA$_{tot}$], b is the rate constant, k_{obs} (s^{-1}), and x is the reaction time, t (*s*). All data were fitted using the nonlinear regression routine in SigmaPlot 9.0 (Systat Software, San Jose, CA, USA). Kinetic data reflect the average of three independent reactions/gel separations and are reported as the mean ± the standard error of the mean.

Results

Assay design

In previous work, monofunctional adducts formed by **1** were shown to inhibit the DNA cleavage chemistry of restriction endonucleases [12]. The restriction sites in which the hybrid agent (but not cisplatin) showed its most pronounced cleavage inhibition were *G*↓AATTC (*Eco*RI) and TTT↓AAA (*Dra*I), where the bases targeted by **1** are italicized and the arrows indicate the sites of endonucleolytic strand scission [12]. For the current study, a 40-base-pair dsDNA fragment was chosen, which contains a central palindromic *Eco*RI restriction site flanked by a 5′ cytidine residue, 5′-*C*GAATTC. Monofunctional platination

of 5′-CGA, a major target sequence of **1**–**4** [12,24,25], occurs at guanine (about 90%) or adenine (about 10%) with the acridine residue intercalating on the 5′ face of the platinated base, i.e., between cytosine and guanine, or between guanine and adenine. We reasoned that the combined effects of these adducts would cause efficient inhibition of *Eco*RI-mediated DNA cleavage and the most pronounced measurable effect in a gel-based assay. Brabec and Balcarova [26] demonstrated in plasmid DNA randomly modified with platinum that although restriction enzyme cleavage is inhibited by adducts within or directly adjacent to the restriction sites, platinated residues at a greater distance are able to slow the recognition of the restriction site by the enzyme. To minimize this effect and to ensure that only cleavage inhibition by adducts localized to the restriction site were detected by the assay, the sequences 5′-CG and 5′GA, as well as other high-affinity sites, were omitted from both strands of the probe sequence. Although this design cannot completely rule out contributions to the inhibitory effect from nonspecific adducts outside the *Eco*RI recognition sequence, it provides a reasonable setup for measuring DNA-binding rates at specific sites in dsDNA.

Polyacrylamide gel electrophoresis analysis of reaction products

The assay was carried out using a setup described previously [22]. Briefly, the radioactively labeled 40-base-pair fragment was incubated under physiologically relevant conditions with excess platinum analogue at a drug-to-nucleotide ratio of 0.1. This corresponds to eight platinum molecules per restriction site, which should saturate the central sequence with inter-calated drug and allow the formation of adducts to be treated as a pseudo-first-order process. Samples were withdrawn from the incubation mixtures at suitable time points, and the reactions were quenched with excess thiourea. Thiourea rapidly replaces the chloro (or aqua) leaving group in unbound complex, rendering platinum unreactive with DNA, but does not reverse existing adducts at 4 °C [12]. The dialyzed samples were then incubated with *Eco*RI, and the reaction products were analyzed by polyacrylamide gel electrophoresis (PAGE). A schematic of the assay and a typical gel generated for compound **2** are shown in Fig. 2. Endonucleolytic cleavage at the restriction site of unmodified probe sequence produces a radiolabeled 18-base-pair fragment (cl. in Fig. 2b) visible on the gel as the band of highest mobility. Using the same incubation conditions, which result in complete scission of the full-length unmodified DNA fragment (f.-l. in Fig. 2b), we treated platinated DNA samples with *Eco*RI and separated the products by denaturing PAGE. With progressing reaction time, a decrease in intensity of the “cl.” band and an increase in intensity of the “f.-l.” band is observed, which is consistent with *Eco*RI inhibition as a consequence of monofunctional adduct formation at the restriction site (Fig. 2b). The third band (cl.-Pt in Fig. 2b), of intermediate mobility, observed on the gels was identified as the 18-base-pair fragment modified with platinum at a remote site (most likely at one of the 5′TG steps [24]) that does not contribute to the cleavage inhibition. When the digested mixtures were incubated with sodium cyanide (NaCN), which removes platinum from DNA, this band coalesces with the “c.l.” band (not shown). However, incubations with NaCN prior to PAGE analysis were avoided in this assay since the high salt concentrations were found to reduce the gel quality, prohibiting accurate band integration.

Kinetic analysis

To extract the reaction rates for each of the derivatives, the relative band intensities at each time point were determined by densitometric integration and normalized to the total intensity across each lane. The procedure is based on the following mechanism (Fig. 3). The hybrid agents bind to DNA via intercalation with micromolar affinity in a rapid, reversible binding step. The agents bind to nucleobase nitrogen at the intercalation site via a prehydrolysis pathway or direct substitution of the chloro leaving group to produce monofunctional adducts, which, if formed at the restriction site, result in quantifiable inhibition of DNA cleavage. The covalent DNA binding step can be intercepted by rapid

replacement of the chloro and/or aqua ligand on platinum with thiourea, preventing the metal from forming irreversible adducts with the biopolymer. Specifically, the treatment of the data is based on the following assumptions and previous observations:

1. At $t = 0$, compounds **1**–**4** bind to the restriction site via intercalation: $[Pt]_0 = [Pt]_{int}$.
2. Conversion of the intercalative adducts into monofunctional adducts is an intramolecular, first-order process and is observed as the sum of the hydrolytic and direct pathways: $k_{obs} = k_{hyd} + k_{dir}$. k_{obs} mainly reflects the rate of platination of guanine.
3. Quenching of the intercalated complex outcompetes DNA adduct formation: $k_q \gg k_{obs}$ [12].
4. *Eco*RI is completely inhibited by adducts formed at the restriction site, and the concentration of resulting uncleaved DNA is equal to the concentration of platinum covalently bound to that site: $[DNA_{f.-l.}] = [Pt_{cov}]$.
5. Non-covalently bound (intercalated) drug does not inhibit *EcoR*RI activity [12].

A representative plot of integrated band intensities versus reaction time for the average of three experiments performed for compound **2** is shown in Fig. 4a. The data plotted for time points ranging from 20 min to 6 h confirm that, as the reaction progresses, the sum of intensities of the bands assigned to cleaved product (cl. + cl.-Pt) decreases at the same rate as the intensity of the full-length band (f.-l.) increases. This observation is consistent with the product (band) assignments and confirms that the concentration of uncleaved probe can be used as a reciprocal measure of the rate at which intercalated drug decays to form covalent adducts. Thus, under (pseudo) first-order conditions, the process of adduct formation can be expressed by the following integrated rate law:

$$\frac{[DNA_{f.-1.}]_t}{[DNA_{tot}]} = a\left(1 - e^{-k_{obs}t}\right), \quad \text{with } a = \frac{[DNA_{f.-1.}]_{max}}{[DNA_{tot}]}, \tag{2}$$

where $[DNA_{f.-l.}]_t/[DNA_{tot}]$ is the fraction (or, if multiplied by 100, the percentage) of probe sequence in which adduct formation at the *Eco*RI restriction site has occurred at time t, and a is the maximum binding level, which can be considered a measure of the relative affinity of a specific derivative for the enzyme's recognition sequence. Three gels were integrated for each compound (**1**–**4**). Average band intensities for the full-length DNA were plotted as "percent protection" against time and fitted to Eq. 2 (Fig. 4b). Kinetic parameters along with previously determined cell growth inhibitory concentrations for each compound are summarized in Table 1. On the basis of these data, the reactivity with the DNA fragment varies significantly among the set of compounds, with binding rates (k_{obs}) and binding levels (a) increasing in the order **4** ≈ **1** < **3** < **2**. Complex **2** shows the highest binding affinity for the sequence and forms adducts at a rate 4 times faster than that observed for the prototype, **1**. A significant ($P < 0.05$) kinetic enhancement by 1.5-fold is also observed for complex **3** relative to complex **1**, whereas complex **4** reacted at a (statistically insignificant) slightly slower rate.

Discussion

Restriction enzyme cleavage inhibition is a sensitive tool for studying the effect of (minor) structural modifications to the prototypical complex, **1**, on the reactivity of the metal with DNA bases. It demonstrates that platinum-acridines react with nucleobase nitrogen considerably faster in dsDNA than in mononucleos(t)ides. For instance, complex **1** binds to guanine-N7 in 2′-deoxyguanosine and in 5′-guanosine monophosphate with half-lives of 4.1

and 3.8 h, respectively [37 °C, excess nucleos(t)ide] [17,22], whereas the half-life determined in this assay is 1.4 h. Likewise, a rate enhancement of the same magnitude is observed for compound **2**, for which half-lives of 65 min and 21 min were determined for reactions with 5′-GMP [22] and dsDNA (this study), respectively. These results demonstrate that the restriction enzyme assay is able to reproduce relative complex reactivities previously determined by NMR spectroscopy. Several effects may contribute to the pronounced increase in binding rate in dsDNA. A high degree of noncovalent preassociation of the cationic agents with the polyanionic DNA, both electrostatic and intercalative, should produce a high effective local concentration of reactive platinum. Furthermore, the geometry of the intercalated complex may facilitate associative substitution by positioning platinum favorably for nucleophilic attack by nucleobase nitrogen. Although platinum(II) typically binds to DNA nitrogen via a prehydrolysis pathway (k_{hyd},Fig. 3) [27], DNA intercalation may catalyze direct substitution of chloride (k_{dir},Fig. 3). This pathway may become dominant as the presence of dsDNA has been shown to slow the aquation rate of the Pt-Cl bond in platinum drugs significantly [28].

Three second-generation derivatives of compound **1** in which functionally important parts of the molecule have been altered were included in this study. In complex **2**, the donor group linking the platinum and intercalator moieties has been changed from a thiourea-sulfur into an amidine-nitrogen group. Complex **3** contains a propane-1,3-diamine (pn) nonleaving group instead of ethane-1,2-diamine (en), and in complex **4** an acridine-4-carboxamide was introduced as a DNA threading intercalator. The most dramatic relative enhancement of DNA-binding rate compared with **1** by approximately fourfold is observed for derivative **2**, which is in agreement with the previously reported DNA binding levels and reactivity of this agent in reactions with 5′-guanosine monophosphate. Reduced steric hindrance and hydrogen-bonding interactions involving the amidine-NH donor group likely contribute to this effect [22]. Replacement of the five-membered en chelate in **1** with a conformationally more flexible six-membered pn chelate in **3** also has a distinct rate-enhancing effect. In a structure- activity relationship study addressing the importance of the nature of the nonleaving group in these complexes, compound **3** was identified as the most active ACRAMTU-based derivative [25]. In the same study, complex **3** was shown, using a PCR-amplified DNA polymerase stop assay, to induce DNA adducts with virtually the same sequence specificity as the prototype, **1** [25]. However, the bands on the sequencing gel were significantly more intense for compound **3** than for compound **1**, which was interpreted to indicate that the pn derivative produces higher adduct levels. This behavior was attributed to steric effects, as an earlier study found that the aquation rate of [$PtCl_2$(diamine)] approximately doubles when the diamine ligand is changed from en to pn [29]. The rate increase by 1.5-fold determined in this study supports these findings. By contrast, derivative **4** was found to react most sluggishly with DNA. Its design promised improved DNA affinity and altered sequence specificity owing to the presence of a groove-binding positively charged 4-carboxamide side chain [24]. Contrary to its design, compound **4** showed the same DNA damage profile as compound **1**, whereas adduct levels were slightly reduced compared with those produced by the prototype. Although the increase in overall charge from 2 + to 3 + should favor DNA binding, slow on/off rates of intercalation, a hallmark of threading intercalators [30], may prohibit rapid covalent binding of the platinum moiety.

The current study demonstrates that the restriction enzyme assay is an efficient tool for probing the kinetics of DNA adduct formation in libraries of structurally related platinum agents. Optimizing the kinetics of platination in these agents seems critical since rapid formation of highly cytotoxic monofunctional adducts has an intrinsic advantage over cross-link formation by the classical platinum drugs. Formation of the GG and AG intrastrand cross-links by cisplatin, the most abundant and putative cytotoxic lesions of this drug, has been studied in DNA and in small model duplexes [27]. The first binding step, which

produces (noncytotoxic) monofunctional adducts, and the subsequent closure to (cytotoxic) bifunctional adducts were shown to proceed with half-lives of approximately 2 h at 37 °C in native DNA [27]. Two-dimensional NMR studies further indicated that the rates of cross-link formation critically depend on whether chelation occurs in the 5′-to-3′or 3′-to-5′ direction at GG and AG sites, which may be slow despite a rapid monofunctional binding step [19,20]. As a consequence, a major population of the intrastrand cross-links may be formed by cisplatin at a rate too slow to be of pharmacological significance. By contrast to the monoadducts formed by cisplatin, which are believed not to contribute to the antitumor effect of the drug, the hybrid adducts of **1**–**4** have to be considered the primary cytotoxic lesion. Since the latter adducts form relatively fast with half-lives determined in this study as short as 21 min for complex **2**, they can be expected to provide a major pharmacodynamic advantage over cisplatin-type cross-links in rapidly proliferating cancer cells. This supposition is supported by the trend in the concentrations required to inhibit cell proliferation by 50% (IC_{50}) determined for compounds **1**–**4** in aggressive H460 lung cancer cells. The binding rates determined in this assay seem to correlate well with the cytotoxic potency of the agents in the lung cancer cell line, but not in HL-60 leukemia cells (Table 1). This observation suggests that in the latter cell line other factors such as altered cellular uptake and platinum detoxification mechanisms may modulate DNA adduct levels and ultimately the biological activity of the complexes. Likewise, inefficient cellular uptake of complex **4** owing to its 3+ charge might explain why this derivative is considerably less active than prototype **1** in both cell lines, even though both agents react with DNA at comparable rates. It will be important to determine if the rate enhancement established for some derivatives in this assay in naked DNA extrapolates to increased platinum levels in nuclear DNA in cancer cells. These studies are underway.

Supplementary Material

Refer to Web version on PubMed Central for supplementary material.

Acknowledgments

This work was funded by the US National Institutes of Health (grant CA101880).

Abbreviations

ACRAMTU	1-[2-(Acridin-9-ylamino)ethyl]-1, 3-dimethylthiourea
dsDNA	Double-stranded DNA
en	Ethane-1,2-diamine
IC_{50}	Concentration required to inhibit cell proliferation by 50%
PAGE	Polyacrylamide gel electrophoresis
pn	Propane-1,3-diamine
Tris	Tris(hydroxymethyl)aminomethane

References

1. Kelland L. Nat Rev Cancer 2007;7:573–584. [PubMed: 17625587]
2. Cepeda V, Fuertes MA, Castilla J, Alonso C, Quevedo C, Perez JM. Anticancer Agents Med Chem 2007;7:3–18. [PubMed: 17266502]
3. van de Vaart PJ, Belderbos J, de Jong D, Sneeuw KC, Majoor D, Bartelink H, Begg AC. Int J Cancer 2000;89:160–166. [PubMed: 10754494]

4. Welters MJ, Fichtinger-Schepman AM, Baan RA, Jacobs-Bergmans AJ, Kegel A, van der Vijgh WJ, Braakhuis BJ. Br J Cancer. 1999;79:82–88.
5. Fujii T, Toyooka S, Ichimura K, Fujiwara Y, Hotta K, Soh J, Suehisa H, Kobayashi N, Aoe M, Yoshino T, Kiura K, Date H. Lung Cancer 2008;59:377–384. [PubMed: 17905465]
6. Martelli L, Di Mario F, Botti P, Ragazzi E, Martelli M, Kelland L. Biochem Pharmacol 2007;74:20–27. [PubMed: 17466278]
7. Lovejoy KS, Lippard SJ. Dalton Trans 2009:10651–10659. [PubMed: 20023892]
8. van Zutphen S, Reedijk J. Coord Chem Rev 2005;249:2845–2853.
9. Baruah H, Barry CG, Bierbach U. Curr Top Med Chem 2004;4:1537–1549. [PubMed: 15579095]
10. Guddneppanavar R, Bierbach U. Anticancer Agents Med Chem 2007;7:125–138. [PubMed: 17266509]
11. Barry CG, Baruah H, Bierbach U. J Am Chem Soc 2003;125:9629–9637. [PubMed: 12904029]
12. Budiman ME, Alexander RW, Bierbach U. Biochemistry 2004;43:8560–8567. [PubMed: 15222767]
13. Baruah H, Day CS, Wright MW, Bierbach U. J Am Chem Soc 2004;126:4492–4493. [PubMed: 15070347]
14. Burstyn JN, Heiger-Bernays WJ, Cohen SM, Lippard SJ. Nucleic Acids Res 2000;28:4237–4243. [PubMed: 11058123]
15. Baruah H, Rector CL, Monnier SM, Bierbach U. Biochem Pharmacol 2002;64:191–200. [PubMed: 12123739]
16. Ackley MC, Barry CG, Mounce AM, Farmer MC, Springer BE, Day CS, Wright MW, Berners-Price SJ, Hess SM, Bierbach U. J Biol Inorg Chem 2004;9:453–461. [PubMed: 15067524]
17. Guddneppanavar R, Wright MW, Tomsey AK, Bierbach U. J Inorg Biochem 2006;100:972–979. [PubMed: 16488016]
18. Brabec V, Christofis P, Slamova M, Kostrhunova H, Novakova O, Najajreh Y, Gibson D, Kasparkova J. Biochem Pharmacol 2007;73:1887–1900. [PubMed: 17400194]
19. Monjardet-Bas V, Chottard JC, Kozelka J. Chem Eur J 2002;8:1144–1150.
20. Davies MS, Berners-Price SJ, Hambley TW. J Inorg Biochem 2000;79:167–172. [PubMed: 10830862]
21. Hegmans A, Berners-Price SJ, Davies MS, Thomas DS, Humphreys AS, Farrell N. J Am Chem Soc 2004;126:2166–2180. [PubMed: 14971952]
22. Ma Z, Choudhury JR, Wright MW, Day CS, Saluta G, Kucera GL, Bierbach U. J Med Chem 2008;51:7574–7580. [PubMed: 19012390]
23. Martins ET, Baruah H, Kramarczyk J, Saluta G, Day CS, Kucera GL, Bierbach U. J Med Chem 2001;44:4492–4496. [PubMed: 11728195]
24. Guddneppanavar R, Saluta G, Kucera GL, Bierbach U. J Med Chem 2006;49:3204–3214. [PubMed: 16722638]
25. Guddneppanavar R, Choudhury JR, Kheradi AR, Steen BD, Saluta G, Kucera GL, Day CS, Bierbach U. J Med Chem 2007;50:2259–2263. [PubMed: 17408248]
26. Brabec V, Balcarova Z. Eur J Biochem 1993;216:183–187. [PubMed: 8365404]
27. Gelasco, A.; Lippard, SJ. Topics in biological inorganic chemistry. Clarke, MJ.; Sadler, PJ., editors. Springer; New York: 1999. p. 1-43.
28. Davies MS, Berners-Price SJ, Hambley TW. Inorg Chem 2000;39:5603–5613. [PubMed: 11151361]
29. Miller SE, Gerard KJ, House DA. Inorg Chim Acta 1991;190:135–144.
30. Wakelin LP, Bu X, Eleftheriou A, Parmar A, Hayek C, Stewart BW. J Med Chem 2003;46:5790–5802. [PubMed: 14667232]

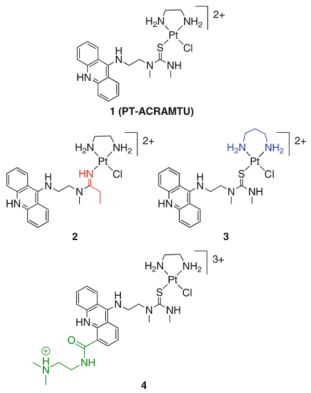

Fig. 1.

Structures of platinum–acridines **1**–**4** with structural modifications in the second-generation derivatives highlighted

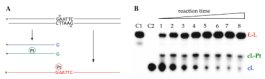

Fig. 2.

a The cleavage inhibition assay. Incubations of the platinum-treated 40-base-pair duplex (*black*) with *EcoRI* and subsequent separation of the mixtures by denaturing polyacrylamide gel electrophoresis (PAGE) results in three detectable products: unmodified (*blue*) and platinum-modified (*green*) 18-base-pair fragments, and uncleaved top strand (*red*). The *asterisks* denote the ^{32}P label, and the *triangles* indicate the sites of endonucleolytic strand scission. **b** Representative denaturing polyacrylamide gel (12% acrylamide, 8 M urea) for the cleavage inhibition assay performed with compound **2**. Lane assignments: *C1* control—unmodified probe sequence; *C2* control—unmodified, *EcoRI*-digested sequence; *1–8* reactions with complex **2** quenched after 20, 40 min, 1, 1.5, 2.5, 3.5, 4.5, and 6 h, respectively, followed by *EcoRI* digestion. The bands are labeled *cl*. for the 18-base-pair fragment, *cl*.-*Pt* for the platinum-containing 18-base-pair fragment, and *f*.-*l*. for the full-length fragment

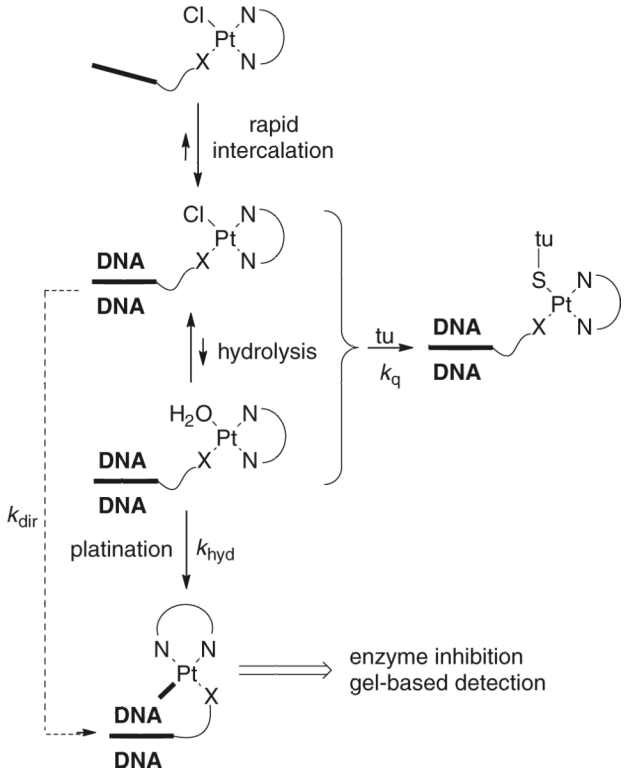

Fig. 3.
Proposed mechanism of monofunctional adduct formation

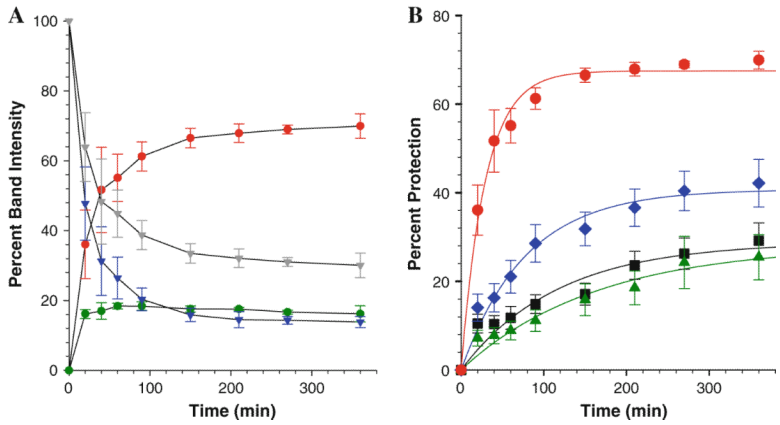

Fig. 4.

a Relative integrated band intensities versus reaction time for compound **2**. The plotted data are the mean (± the standard deviation) of three individual experiments (gels). Trace assignments: *red* uncleaved, full-length fragment (f.-l.); *blue* cleaved 18-base-pair fragment (cl.); *green* cleaved, platinum-containing 18-base-pair fragment (cl.-Pt); *gray* calculated sum of "cl." and "cl.-Pt" band intensities. **b** Intensities of the "f.-l." band versus reaction time for compounds **1** (*black*), **2** (*red*), **3** (*blue*), and **4** (*green*). Each data point is the mean of three individual experiments, with error bars representing ±the standard error of the mean. The *solid lines* represent calculated best fits to Eq. 2 based on the first-order approximation (see the text)

Table 1

Summary of kinetic and biological data

Compound	$k_{obs} \times 10^4 \pm$ SD (s^{-1})[a]	$a \times 100 \pm$ SD (%)	$t_{1/2}$ (min)	$IC_{50,H460}$ (μM)	$IC_{50,HL\text{-}60}$ (μM)
1	1.4 ± 0.37	29 ± 3	83 ± 22	0.35[b]	2.8[b]
2	5.7 ± 0.58	68 ± 2	21 ± 2	0.028[b]	3.0[b]
3	2.1 ± 0.40	41 ± 3	55 ± 10	0.078[c]	3.9[c]
4	1.1 ± 0.40	28 ± 5	104 ± 38	6.1[d]	10.6[d]

Data were obtained through cell proliferation assays. IC_{50} is the concentration required to inhibit cell proliferation by 50% *SD* standard deviation

[a] At 37 °C, pH 7.5

[b] See [22]

[c] See [25]

[d] See [24]